

Interaction of ultrasonic waves with partially-closed cracks in concrete structures

Pahlavan, Lotfollah; Zhang, F.; Blacquière, Gerrit; Yang, Yuguang; Hordijk, Dick

DOI

[10.1016/j.conbuildmat.2018.02.098](https://doi.org/10.1016/j.conbuildmat.2018.02.098)

Publication date

2018

Document Version

Final published version

Published in

Construction and Building Materials

Citation (APA)

Pahlavan, L., Zhang, F., Blacquière, G., Yang, Y., & Hordijk, D. (2018). Interaction of ultrasonic waves with partially-closed cracks in concrete structures. *Construction and Building Materials*, 167, 899-906. <https://doi.org/10.1016/j.conbuildmat.2018.02.098>

Important note

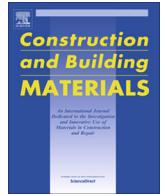
To cite this publication, please use the final published version (if applicable). Please check the document version above.

Copyright

Other than for strictly personal use, it is not permitted to download, forward or distribute the text or part of it, without the consent of the author(s) and/or copyright holder(s), unless the work is under an open content license such as Creative Commons.

Takedown policy

Please contact us and provide details if you believe this document breaches copyrights. We will remove access to the work immediately and investigate your claim.



Interaction of ultrasonic waves with partially-closed cracks in concrete structures

Lotfollah Pahlavan^{a,*}, Fengqiao Zhang^{a,b}, Gerrit Blacquièrè^c, Yuguang Yang^b, Dick Hordijk^b

^a Department of Structural Reliability, TNO, Delft, The Netherlands

^b Department Structural Engineering, Delft University of Technology, Delft, The Netherlands

^c Department of Acoustics and Sonar, TNO, The Hague, The Netherlands

HIGHLIGHTS

- The interaction of ultrasonic waves with partially-closed cracks in concrete has been studied.
- The influence of crack opening and incident angle on the signal features has been evaluated.
- The width of the crack process zone has been estimated from the data.
- The anisotropy of the material at the crack zone has been quantified.

ARTICLE INFO

Article history:

Received 31 July 2017

Received in revised form 15 January 2018

Accepted 14 February 2018

Available online 23 February 2018

Keywords:

Ultrasonic elastic waves

Concrete beam

Crack

Anisotropy

ABSTRACT

Interaction of ultrasonic waves with partially-closed surface-breaking cracks in concrete structures has been studied. Measurements have been conducted on a reinforced concrete beam containing various mechanical-load-induced cracks and compared with the baseline measurements at those locations. Influence of crack width, incident angle of waves with cracks, and distance from the cracks on travel time and amplitude of the waves have been investigated when the beam was unloaded. It has been observed that a measurable part of the waves propagate through the cracks due to the acoustic coupling between the crack faces, although attenuation can be relatively high. The travel time has shown a nearly independent behavior from remaining crack opening in the measured range of 0.05 mm to 3 mm. Measurements in directions orthogonal and parallel to the crack suggest that there is substantial anisotropy in the cracking zone. Furthermore, an effective width of the micro-cracking area around the cracks has been estimated from the measurements.

© 2018 Elsevier Ltd. All rights reserved.

1. Introduction

Surface-breaking cracks commonly occur in concrete structures. In reinforced concrete, development of such cracks can lead to increased risk and rate of corrosion by facilitating the transfer of corrosive substances to the reinforcement bars [4,7]. Proper identification and characterization of these cracks may therefore provide valuable input for improved assessment of structural reliability and durability of concrete structures.

Ultrasonic elastic-wave methods form an important class of non-destructive assessment techniques for concrete structures. Extensive investigations have been reported on characterizing the effect of cracks on ultrasonic waves in such media, see for example Liu et al. [9], Zerwer et al. [19], Shin et al. [17], Popovics

et al. [14], Masserey and Mazza [10], Kee and Zhu [8], and Aggelis et al. [2]. Tomographic methods, as an example of a multi-dimensional assessment technique based on ultrasonic waves, have been implemented in various studies [5,16,1,18,3,15] in which the distribution of material stiffness is estimated from the distribution of speed of sound using an inversion scheme based on several pitch-catch measurements. Despite all the promising achievements, the majority of the reported methods are, in the kernel, either based on an idealized analogy of cracks to perfect notches, i.e. voids, or consider a simplified angle-independent transmission mechanism for ultrasonic waves through the cracks, due to which some inconsistencies in the reported observations can be identified. The acoustic coupling extent and details between the crack faces are expected to have a major effect on the diagnostic signals. For example, a perfect notch model is associated with strong scattering of the waves by the crack and diffraction from the crack tip, while a transmission model is associated with

* Corresponding author.

E-mail address: pooria.l.pahavan@gmail.com (L. Pahlavan).

possibly-angle-dependent attenuation and time delay when the waves pass through the cracks. While there is general consensus that open cracks under substantial tensile stress can be described by the former model, closed and partially-closed cracks have been shown to allow a notable signal transmission [8]. For field application of elastic-wave-based assessment techniques and to minimize the contamination of the data with background noise, a particular situation of partially-closed cracks in the absence of excessive loads is of special interest (misalignment of aggregates may not allow perfect crack closure). The behavior of these cracks, to the extent that is desirable for application in a generic damage diagnosis method such as tomography, does not seem to have been sufficiently studied.

In this paper, a detailed investigation of the interaction of ultrasonic waves with imperfectly-closed cracks in an unloaded beam is presented. The designed experiments comprised five sets of measurements to quantitatively study: (i) the coupling variation of transducers, (ii) the baseline properties of the test sample, (iii) the influence of crack (remaining) opening on the signal features, i.e. amplitude and arrival time, (iv), the anisotropy in the crack zone, and (v) the effective width of the crack process zone. In each set, the responses have been compared to the baseline signal, i.e. the signal obtained when no defect was present. The results suggest that careful consideration of the crack behavior is essential in the development of passive and active elastic-wave-based techniques for assessment of existing concrete structures, such as acoustic emission and elastic-wave tomography.

2. Description of measurements

A brief theoretical background of the assessment approach is presented in this section. In order to study the effect of cracks on the diagnostic ultrasonic waves, a number of experiments have been designed and performed such that in each measurement set, a reference signal, i.e. baseline, is recorded alongside the signal influenced by the crack. For this, three transducers are used in each measurement, where one is transmitter and the other two are receivers, as schematically shown in Fig. 1. The receivers are placed at the same distance but opposite from the source.

When the transmitter coupled to the structure surface emits an ultrasonic pulse, it propagates inside the medium and on its surface. The recorded responses, i.e. the convolution of the source pulse transmitted into the concrete medium, the transfer function of the medium between the source and the receiver, and the transfer function of the receiver apparatus, at the two receiver locations (denoted by P_1 and P_2) can be described in the frequency domain as:

$$P_1(\omega) = \sum_i D_1^i(\omega) W^{ii}(l, \omega) S^i(\omega), \forall i \in [P, S, R, H], \quad (1)$$

$$P_2(\omega) = \sum_j \sum_i D_2^j(\omega) [\bar{W}^{ji}(l, \omega) + \tilde{W}^{ji}(l, \omega)] S^i(\omega), \forall i, j \in [P, S, R, H], \quad (2)$$

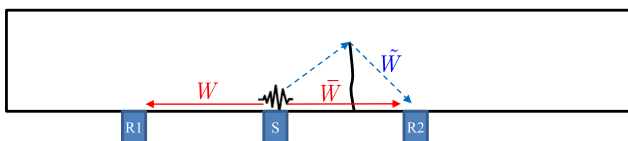


Fig. 1. Schematic illustration of the ultrasonic source (S) and receivers (R1 and R2) on the concrete member. In all the experiments, the transducers are placed such that a single crack under investigation is located between the source and one of the receivers.

where ω is the radial frequency, the superscript i and j denote the wave mode (each can denote pressure, shear, Rayleigh, and head waves), D_k^i is the transfer functions of receiver k for wave mode i , W^{ii} is the transfer function of the medium without crack for wave mode i , \bar{W}^{ij} is the transfer function for waves entering the crack zone as mode i and leaving it as mode j , \tilde{W}^{ij} is the transfer function for waves diffracted and possibly mode converted by the crack tip, l is the distance between the source and each receiver (similar in this case), and $S(\omega)$ denotes the generated pulse. The transfer function of the medium with crack may be simplified as:

$$\bar{W}^{ji}(l, \omega) = W^{ji}(l - l_c, \omega) Q^{ji}(l_c, \phi, \omega) \quad (3)$$

with Q the transfer function of the medium in the crack process zone affected by micro-cracking with effective length l_c . While W is a function of the base material properties and composition, $Q(l_c, \phi)$ can additionally depend on crack depth, transparency, and incident angle ϕ . These transfer functions may be obtained experimentally, analytically, or numerically.

For the comparison of the signals of the baseline and cracked cases to be meaningful, the coupling terms, i.e. D_1 and D_2 , should be reasonably similar. The first set of the measurements in this research was hence dedicated to the quantification of coupling variation. The second set dealt with extraction of the properties of the medium (related to transfer function W) using an array of transducers. This information was necessary for estimation of the wave speed in the damaged area (related to transfer function Q) at a later stage. In the next measurement set, the influence of the crack opening on the signal amplitude and arrival time was studied (related to Q). Furthermore, the extent of the damage zone at the crack vicinity was assessed (related to l_c), followed by an assessment of the directional properties of the cracks (also related to Q).

3. Experiments

A reinforced concrete beam with length, height, and depth of 10 m, 0.8 m, and 0.3 m, respectively, which hosted several cracks of different opening and orientation, was chosen. The concrete class was C65 with compressive strength of about 68 MPa, and the maximum aggregate size was 16 mm. The cracks were generated in a shear test (not shown) under excessive loading, as schematically illustrated in Fig. 2. The beam was unloaded and placed on the floor of the laboratory, as can be seen in Fig. 3. A number of cracks with different remaining openings ranging from 0.05 m to 3 mm, which were measured with a crack width ruler on the beam surface, were selected for the ultrasonic tests. The data acquisition system was Sensor Highway II by MISTRAS, and the transducers were of resonant type with center frequencies of 60 kHz and 150 kHz, i.e. R6I and R15I, from the same vendor, used as both transmitter and receiver. The transducers were attached to the surface using a viscoelastic adhesive couplant.

3.1. Coupling sensitivity

Several measurement sets were performed to investigate the variation in the coupling of the transducers. To maintain the source signal constant at each set, four R6I transducers were placed on a circular pattern at a distance of 106.5 mm from the source, i.e. standard pencil lead break. This experiment was repeated 6 times at the same location on the beam by removing and re-installing the transducers.

3.2. Baseline properties

An array of 14 R6I transducers was mounted on the surface of the structure in an area without cracking. The spacing between

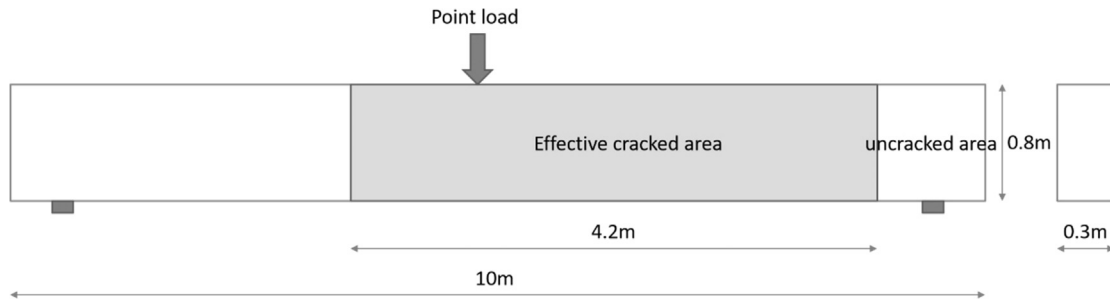


Fig. 2. Dimensions of the test beam.

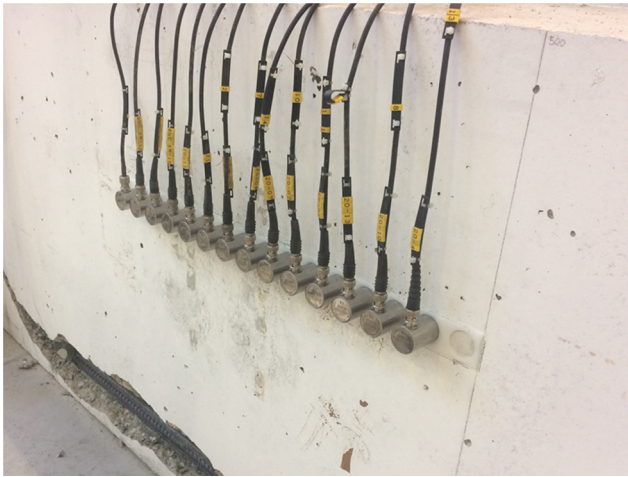


Fig. 3. Baseline measurements with an array of 14 transducers.

the transducers was 40 mm ensured by a thin plastic mold, as shown in Fig. 3. Transducer 1 (the first from left in Fig. 3) was used as a source element, excited with a rectangular-shape pulse of 20 μs duration and 10 V amplitude. The induced pulse in the medium can therefore be considered as the convolution of this pulse with the narrow-band transfer function of the transducer and the coupling layer.

3.3. Crack width influence

A number of cracks with openings of 0.05 mm, 0.1 mm, 0.2 mm, 0.3 mm, 0.6 mm, 1 mm, 1.5 mm and 3 mm (measured at the surface of the unloaded beam) were found and chosen, as can be partly seen in Fig. 4. Two receivers were placed at a distance of 80 mm from the source, in such a way that one of the source-receiver paths contained a crack. The source signal was the short-duration pulse described in Section 3.2. With the cracks all the way through the beam, the positioning of the transducers relative to the cracks was considered such that for the first-arriving wave packet, the possibility of travelling through could be distinguished from the possibility of diffraction from the tip of the cracks. To exemplify, with a distance of 150 mm from the crack tip to the transducers, the tip-diffracted terms (captured by \dot{W}^{ij} in Eq. (2)) are expected to appear with more than 53 μs delay compared to the baseline signal (considering maximum speed of 4100 m/s). Longer time delays are associated with larger distances, e.g. 102 μs delay for 250 mm distance. If notable changes to the signal occur before the diffracted waves are expected, they can be attributed to the part passing through the crack.

In the conducted experiments, the minimum distance of transducers from the crack tip was predominantly larger than 200 mm

(expect for the case of 0.05 mm crack which had a distance around 100 mm, due to practical limitations). The measurements were carried out with both 60 kHz (R6I) and 150 kHz (R15I) transducers.

3.4. Crack zone (band) width

Concrete cracking has been reported to be associated with a so-called fracture process zone, leaving a network of micro-cracks around the main crack and causing reduced stiffness. The width of this zone has been investigated by various researchers, for example [11,13,12]. In this set of measurements, the compatibility of this notion with measured ultrasonic signals is evaluated. Similar to the previous set, R6I transducers with spacing of 80 mm were applied on the crack with 0.6 mm opening. In order to estimate the effective width of the area affected by micro-cracks (characterized by reduced stiffness and hence speed of sound), the source and one of the receiver transducers have been initially placed on the crack trajectory, and further moved away from it without changing the orientation, as shown Fig. 5. The third transducer to measure the baseline signals was placed in the orthogonal direction.

3.5. Anisotropy in the crack zone

From the conducted measurements parallel and orthogonal to the crack, the anisotropy of the medium at the crack zone can be estimated. R6I transducers were utilized in this experiment on the crack with opening of 0.6 mm. The distance between the transducers was 80 mm, similar to the previous experiment.

4. Results and discussion

The waveforms from all the experiments were acquired at a sampling rate of 1 MHz, and with a trigger time of 256 μs . The processing was performed in the time domain in a consistent manner to the commonly-used approach in tomography and acoustic emission techniques, i.e. the onset of the first-arriving wave was determined based on exceeding a predetermined threshold, and subsequently registering the amplitude of the first peak. Care should be taken to deal with interference of the first arrival with other wave modes and boundary reflections, e.g. by placing the transducers at a sufficient distance from the edges of the beam. Processing of the signals in the time domain implies that a range of frequencies are mixed in the analysis of signal amplitudes, however, given the reasonably-narrow band of the transfer function of the transducers (effectively between 40 kHz and 90 kHz), this is believed to be an acceptable processing domain.

It is also noted that the transfer function of the sensors of the same type are nearly similar, but not exactly identical. This also holds for the couplant layer. As a result, the transmitted source signals into the medium have been observed to be similar during the first 50 μs of excitation, and only after that the difference becomes

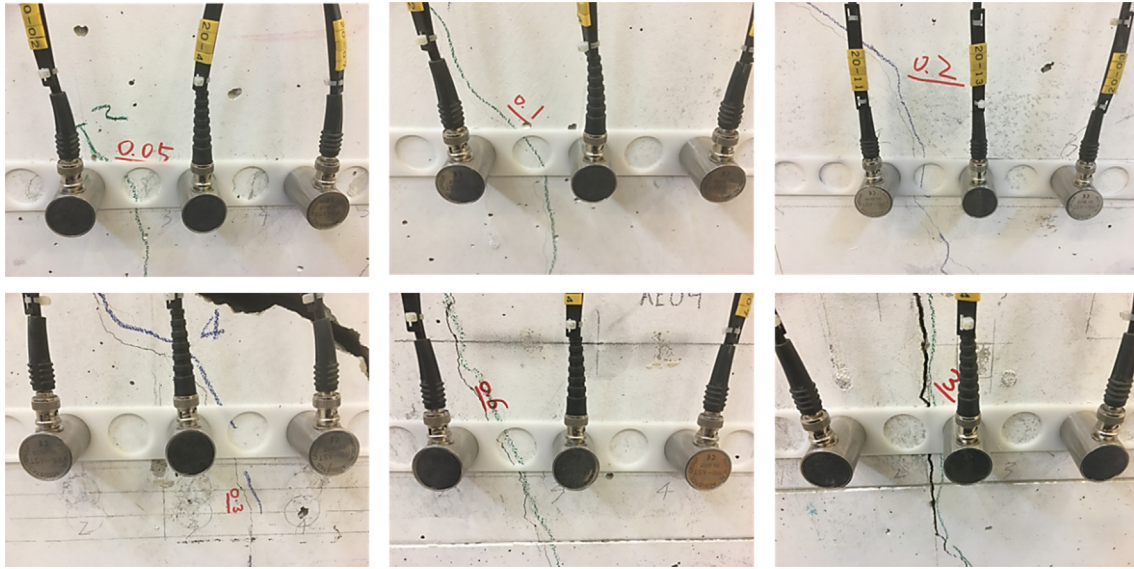


Fig. 4. Measurements on crack width influence in the range 0.05–3 mm.



Fig. 5. Measurements on the influence of distance to crack (left and middle) and crack orientation (right).

notable. The duration of $50 \mu\text{s}$ encompasses the excitation peak and hence serves the purpose for this investigation.

4.1. Coupling variation

The total variation in the amplitude of the received signals in the repeated measurements turned out to be limited to 5 dB, with proper control of the thickness of the adhesive layer. This means that the results shown in the remainder of this paper when discussing the signal amplitudes are subject to this level of variation. Note that no major phase variation was observed in this analysis.

4.2. Baseline characterization

Using the array of transducers, the signal transmitted by element 1 was acquired with the rest of the elements. With the transmitter and receiver placed on the same surface, surface Rayleigh (R) and head waves, i.e. refracted P waves, are predominantly measured. With a trigger time of $256 \mu\text{s}$, the response acquired by the first 6 receivers was used to extract the speed of R and P waves, as shown in Fig. 6. With the relatively small distances chosen with regard to the relatively high attenuation, interference of these wave modes was inevitable. To minimize this adverse interference effect on the accuracy and given the larger amplitude of the R waves, the velocity of P waves was determined from the onset of the recorded waves, while the peak amplitude of the R waves was used to estimate their speed (best fitted line). From this anal-

ysis and as graphically illustrated, velocities of 4100 m/s and 2400 m/s were extracted for the P and R modes, respectively.

Note that in the considered configuration, a larger uncertainty is associated with the estimated speed of the R waves, not only due to the mode interference (for example more strongly pronounced in transducers 1 and 5, i.e. a1 and a5), but also because of the possible differences in the transfer functions of the transducers (as discussed previously). These can lead to variations in the signal shape and its peak time. The procedure for the onset picking of the P waves, on the other hand, desirably stable.

4.3. Effect of crack opening

The raw data acquired for the 8 cracks with openings between 0.05 mm and 3 mm is shown in Fig. 7. The signals amplitudes have been normalized with respect to the maximum amplitude of the baseline signals. In the baseline response, the peak occurred around $310 \mu\text{s}$, after which interference with other scatterings and diffractions (including boundary reflections) were also picked up. Given the positioning of the transducers with respect to the cracks and the relatively small time delays compared to the baseline (see Section 3.3), the first arriving wave packet was concluded to have travelled through the cracks (and not diffracted from their tips). In the presence of cracks, the amplitude of the signal is observed to drop substantially and a delay is introduced in the arrival time of the signals, as discussed more elaborately here.

Dependence of the onset of the first-arriving wave packet, i.e. P waves, and the amplitude of the dominant R waves (see Section 4.2)

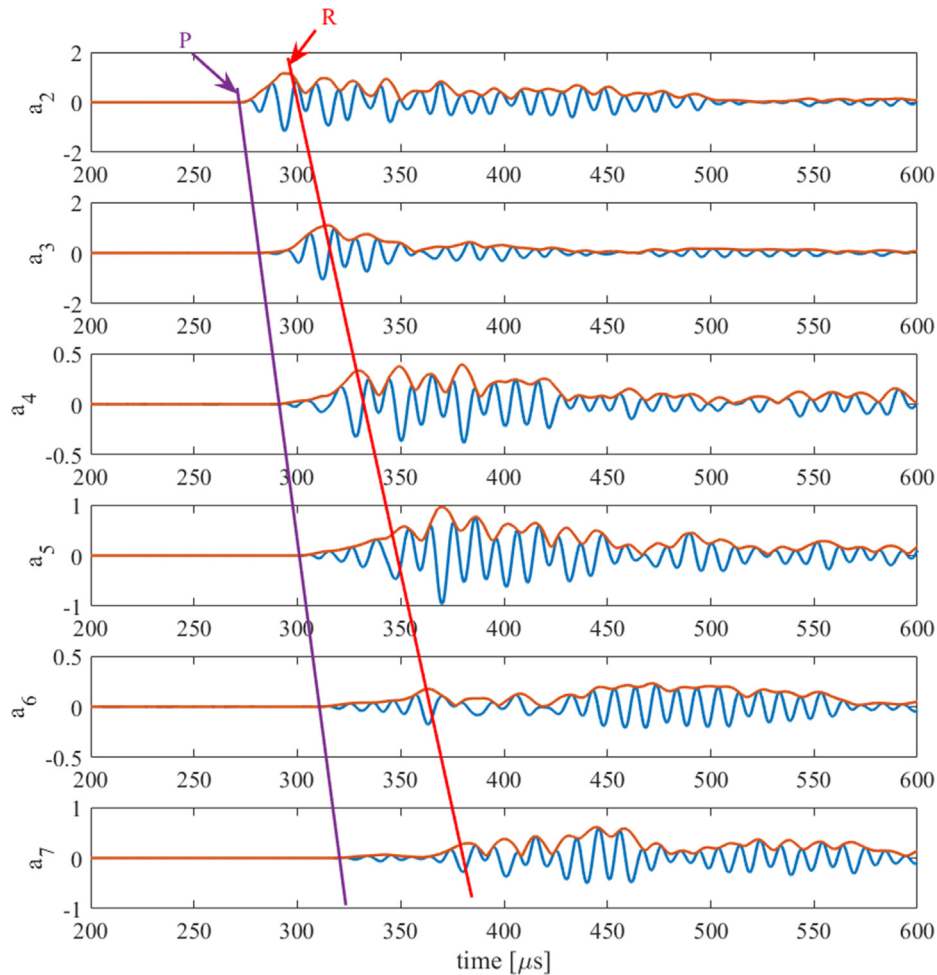


Fig. 6. Estimation of the speed of P and R waves from the 7 transducers in an array with 20 mm spacing: the estimated velocities of P and R waves from the signals are about 4100 m/s and 2400 m/s.

on crack opening have been shown in Fig. 8 (left) and Fig. 9 (left) when R6I transducers were used. For onset picking, a threshold of 1% of the signal maximum amplitude was applied. For amplitude selection, a window length of 50 μs starting from the detected onset was applied to exclude possibly other scattered and mode-converted waves as much as possible. The travel time delay does not exhibit a particular trend with respect to the crack width, and oscillates around 20 μs with an uncertainty band of about 13 μs (which would be about 6 μs if the 0.1 mm crack is excluded). The amplitude decay of the signal seems to increase with the crack opening, suggesting a variation in the range of 10–50 dB. With a relatively large uncertainty band of ± 12 dB, this amplitude drop may be considered inversely proportional to the logarithmic crack opening. The uncertainties in the arrival time and amplitude is expected to partly originate from the variations in the incident angles (see Fig. 4 and also from the detailed interface condition between the crack faces (no two cracks are identical). In addition, coupling variation in mounting the transducers and local variation of material properties, i.e. heterogeneity, also contribute to the uncertainty. Nevertheless, these approximations may be insightful for interpretation of elastic-wave tomography results on concrete samples.

The measurements were repeated using R15I transducers, and the results can be seen in Fig. 8 (right) and Fig. 9 (right). Both the arrival times and amplitudes showed comparable trends to the ones observed from the R6I transducers. The smaller uncer-

tainty in this experiment (compared to the one with R6I transducers) is partly attributed to the more careful angular positioning of the transducers with respect to the crack, and partly to the frequency-dependent transmission behavior of the crack, possibly to a smaller extent.

The implications of the observed influence of crack opening on the signal features can be discussed in different contexts, e.g. elastic-wave tomography and acoustic emission. For elastic wave tomography, these results suggest that merely measuring the travel times of the waves does not provide sufficient information for characterization of the cracks. Merely measuring the amplitudes, on the other hand, may be associated with undesirably large uncertainties for the characterization process. Analysis schemes based on both travel time and amplitude are accordingly recommended for elastic-wave tomography. In the context of acoustic emission, the observed behavior of cracks imply that the presence of existing cracks does not only adversely influence the accuracy of source localization (because of additional time delays in the recorded signals), but also the reliability of the measurement system. When signal amplitudes drop substantially between an acoustic emission source, e.g. an active crack, and the receivers due to other existing cracks on the way, the resulting signal may go below the threshold of the measurement system thereby completely missing the event. These issues are considered as important topics for the future research.

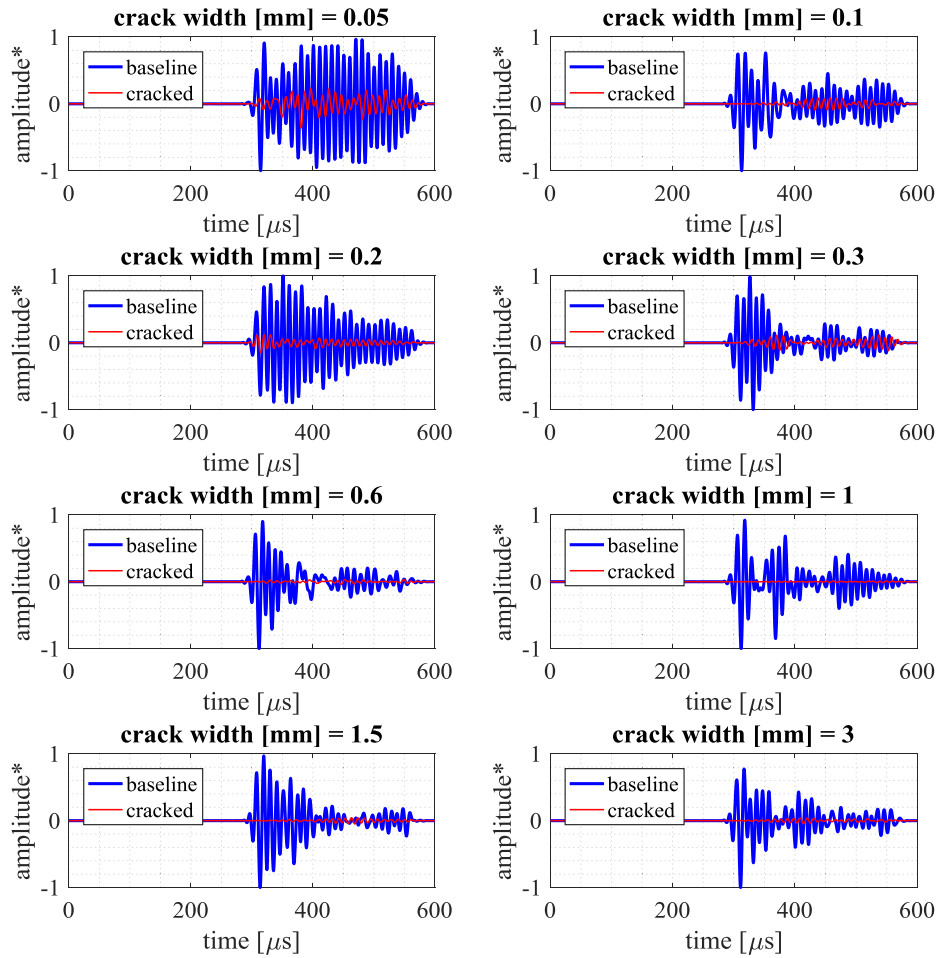


Fig. 7. The raw signals obtained from crack width measurements using R6I.

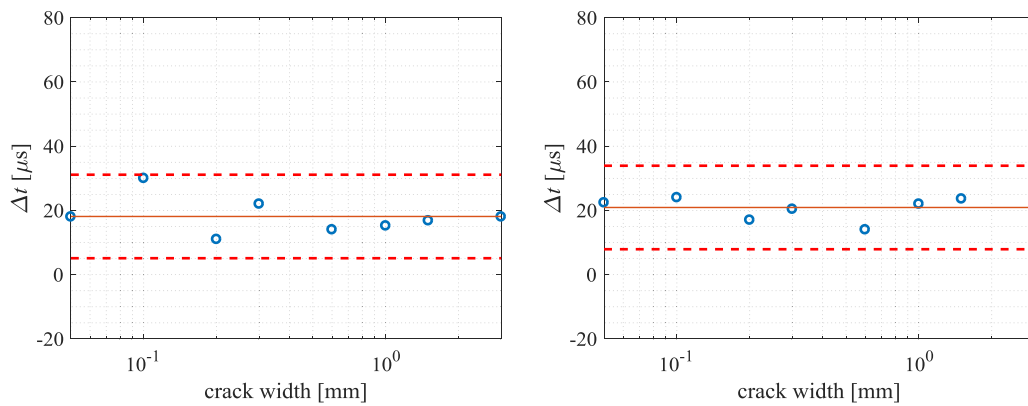


Fig. 8. Dependence of travel-time difference on crack width captured with R6I (left) and R15I (right) transducers.

4.4. Effect of distance from crack

Measurements were carried out on the crack with 0.6 mm opening, with the pair of transmitter–receiver parallel to the crack and at distances of 0, 10 mm, 20 mm, and 40 mm (between the center of the transducers and the crack face), see Fig. 5 (left). The signals are shown in Fig. 10. At each set, a baseline signal has also been acquired at the same distance, but in the orthogonal direction to the crack. The signals are expected to be least affected when the direct path is predominantly outside the fracture process zone

including micro-cracks. Although some refraction and reflection by the main crack surfaces may also be present, the extent of these components is deemed reasonably small. Both travel time and amplitude of the signals are studied here.

The variation of signal arrival time with respect to the baseline as a function of the distance from the crack has been shown in Fig. 11. The maximum time difference was about 5 μs and observed when the transducers were placed directly on the crack. The arrival time difference decreased monotonically with the distance. From the small difference of about 2 μs at distance of 20 mm, which fur-

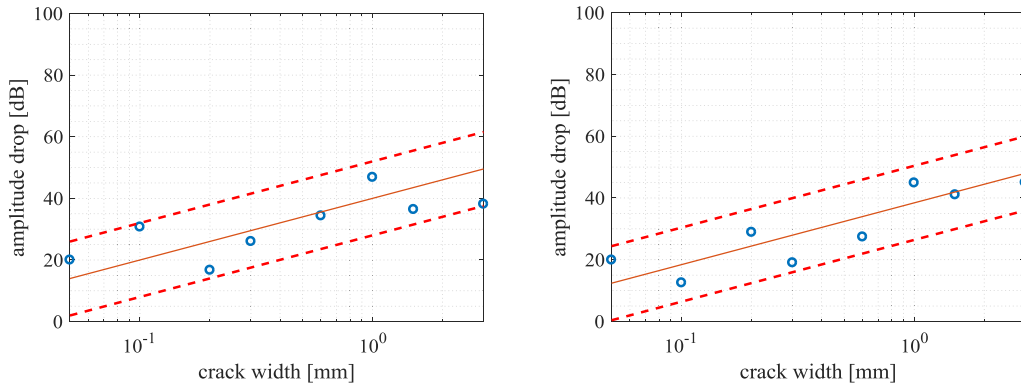


Fig. 9. Dependence of signal amplitude on crack width captured with R6I (left) and R15I (right) transducers.

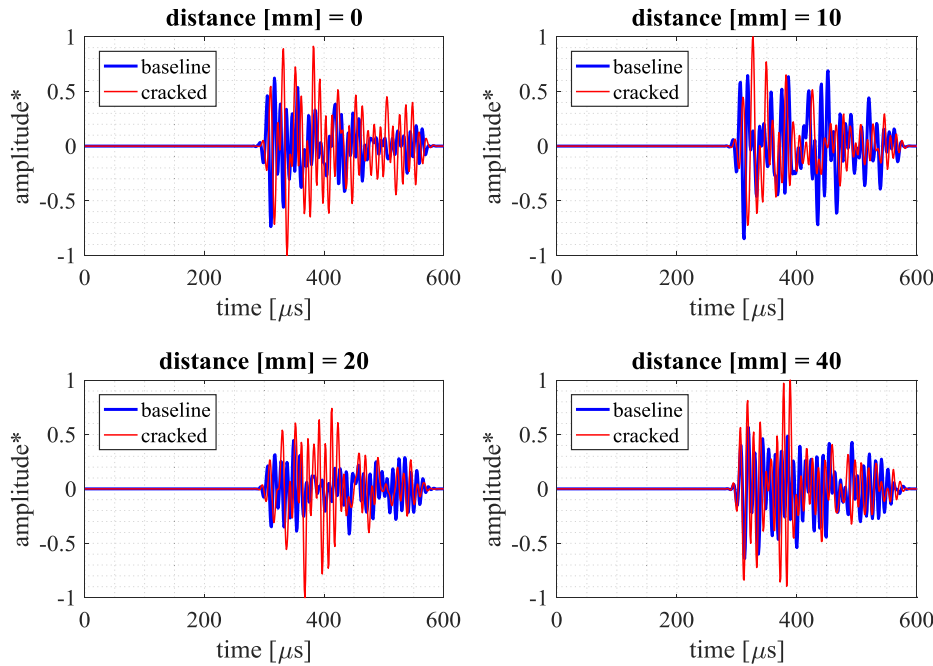


Fig. 10. The raw signals obtained from crack-distance influence measurements.

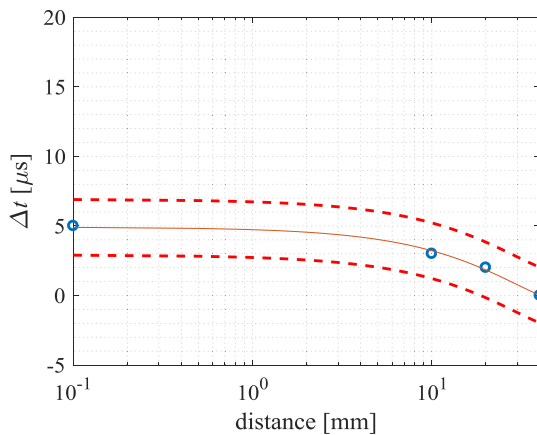


Fig. 11. Dependence of travel-time difference on the distance from the crack with R6I transducers.

ther vanished at the distance of 40 mm, it may be concluded that the micro-cracking area extends slightly beyond 20 mm one-

sided, and therefore 40 mm in total, which coincides reasonably with the previously reported ranges of 2.5–3 times the maximum aggregate size. Note that extraction of the exact value of crack zone width is not feasible in this case since the transducers are not point-contact (diameter is about 29 mm).

The variation of signal amplitude with the distance from the crack was also investigated, as shown in Fig. 12. However, no notable dependence was observed as the variation is in the range of the expected coupling variation.

4.5. Anisotropy

In the directions orthogonal and parallel to the crack travel time differences of 20 μs and 5 μs were observed, respectively, over a traveling distance of 80 mm for the surface head waves with nominal speed of 4100 m/s, i.e., in the undamaged area. Assuming a crack band width of 48 mm with uniform properties, the speed that would explain the 20 μs difference is about 1500 m/s (about 37% of the baseline speed). Assuming constant density at the crack zone, this speed suggests that the Young modulus in the orthogonal direction is approximately 13% of the baseline one. In the par-

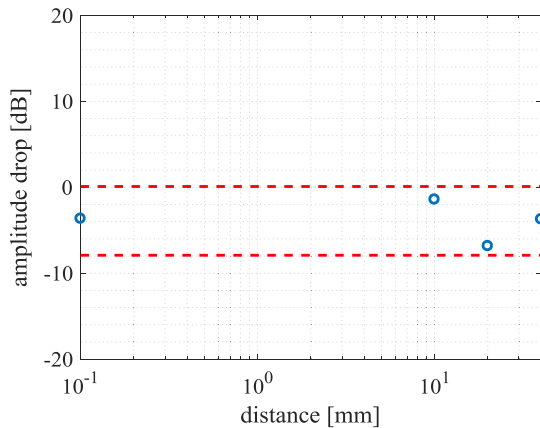


Fig. 12. Dependence of signal amplitude on the distance from the crack with R6I transducers.

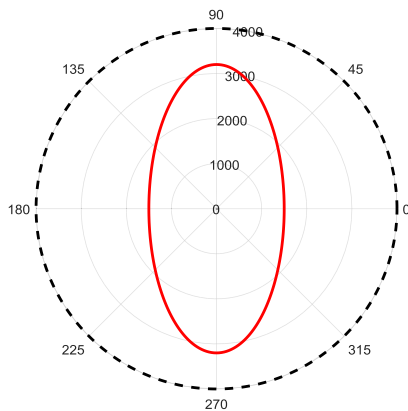


Fig. 13. Anisotropy at the crack zone measured with R6I transducers. The measurement points are along 0 and 90°, and the rest has been interpolated based on an elliptical anisotropy assumption.

allel direction, the speed that explains the 5 μ s difference would be 3260 m/s (about 80% of the baseline speed). Assuming constant density, this suggests that the Young modulus in the parallel direction is approximately 63% of the baseline one.

For graphical illustration and using an elliptical anisotropy model [6], the interpolated speed of P wave as a function of angle has been given in Fig. 13. Other choices for the anisotropy model and additional validation points are to be considered for the future research.

The strong anisotropy observed at the crack location and the generally-unknown angular positioning of cracks in concrete structures suggest that consideration of a full anisotropic model may be necessary in elastic-wave tomography formulations. Furthermore, in the context of conventional acoustic emission, this issue is expected to be a contributing factor to the total localization error.

5. Conclusion

From measurements conducted on a concrete beam with maximum aggregate size of 16 mm and various imperfectly-closed cracks in the range from 0.05 mm to 3 mm from a previously-performed load test, it was observed that both amplitude and travel time of ultrasonic waves are generally affected in interaction with cracks. A travel time difference of about 20 μ s was observed when waves travelled through the cracks, without any notable

trend with respect to the remaining crack opening. Substantial amplitude drop predominantly in the range from 10 dB to 50 dB was also observed. It is concluded that strong anisotropy exists in the crack zone, with the wave speeds in the orthogonal and parallel directions being about 37% and 80% of the baseline values, respectively. Furthermore, the evaluated width of 40 mm for the micro-cracking area at the crack vicinity coincides with the previously-reported range of 2.5–3 times the maximum aggregate size for fracture process zone.

The results of this research may in the future be used in formulation of hybrid tomography schemes based on both amplitude and time delay of the signals in anisotropic media to more accurately characterize cracks in concrete. Furthermore, improved procedures for acoustic emission analysis may be derived based on the disclosed local interaction of elastic waves with existing closed cracks located between the signal source and the receivers.

Acknowledgment

This work has been conducted in the framework of research program ‘ERP-Structural Integrity’ at TNO, in collaboration with Department Structural Engineering of Delft University of Technology.

References

- [1] D.G. Aggelis, T. Shiotani, Repair evaluation of concrete cracks using surface and through-transmission wave measurements, *Cem. Concr. Compos.* 29 (9) (2007) 700–711.
- [2] D.G. Aggelis, T. Shiotani, D. Polyzos, Characterization of surface crack depth and repair evaluation using Rayleigh waves, *Cem. Concr. Compos.* 31 (1) (2009) 77–83.
- [3] A. Behnia, H.K. Chai, M. Yorikawa, S. Momoki, M. Terazawa, T. Shiotani, Integrated non-destructive assessment of concrete structures under flexure by acoustic emission and travel time tomography, *Constr. Build. Mater.* 67 (Part B) (2014) 202–215.
- [4] L. Bertolini, B. Elsener, P. Pedferri, R. Polder, *Corrosion of Steel in Concrete: Prevention, Diagnosis Repair*, 2005.
- [5] L.J. Bond, W.F. Kepler, D.M. Frangopol, Improved assessment of mass concrete dams using acoustic travel time tomography. Part I - theory, *Constr. Build. Mater.* 14 (3) (2000) 133–146.
- [6] P.F. Daley, F. Hron, Reflection and transmission coefficients for seismic waves in ellipsoidally anisotropic media, *Geophysics* 44 (1) (1979) 27–38.
- [7] C.A. Issa, P. Debs, Experimental study of epoxy repairing of cracks in concrete, *Constr. Build. Mater.* 21 (1) (2007) 157–163.
- [8] S.H. Kee, J. Zhu, Surface wave transmission across a partially closed surface-breaking crack in concrete, *ACI Mater. J.* 111 (1) (2014) 35–46.
- [9] P.L. Liu, K.H. Lee, T.T. Wu, M.K. Kuo, Scan of surface-opening cracks in reinforced concrete using transient elastic waves, *NDT E Int.* 34 (3) (2001) 219–226.
- [10] B. Masserey, E. Mazza, Analysis of the near-field ultrasonic scattering at a surface crack, *J. Acoust. Soc. Am.* 118 (6) (2005) 3585–3594.
- [11] H. Mihashi, N. Nomura, S. Niiseki, Influence of aggregate size on fracture process zone of concrete detected with three dimensional acoustic emission technique, *Cem. Concr. Res.* 21 (5) (1991) 737–744.
- [12] K. Ohno, K. Uji, A. Ueno, M. Ohtsu, Fracture process zone in notched concrete beam under three-point bending by acoustic emission, *Constr. Build. Mater.* 67 (2014) 139–145.
- [13] K. Otsuka, H. Date, Fracture process zone in concrete tension specimen, *Eng. Fract. Mech.* 65 (2) (2000) 111–131.
- [14] J.S. Popovics, W.J. Song, M. Ghandehari, K.V. Subramaniam, J.D. Achenbach, S.P. Shah, Application of surface wave transmission measurements for crack depth determination in concrete, *ACI Struct. J.* 97 (2) (2000) 127–135.
- [15] X. Qi, R. Hao, Improved algorithm based on block iteration for ultrasonic computerized tomography on concrete, *J. Inf. Comput. Sci.* 12 (11) (2015) 4377–4384.
- [16] J. Rhazi, Evaluation of concrete structures by the acoustic tomography technique, *Struct. Health Monit.* 5 (4) (2006) 333–342.
- [17] S.W. Shin, J. Zhu, J. Min, J.S. Popovics, Crack depth estimation in concrete using energy transmission of surface waves, *ACI Mater. J.* 105 (5) (2008) 510–516.
- [18] T. Shiotani, H. Ohtsu, S. Momoki, H.K. Chai, H. Onishi, T. Kamada, Damage evaluation for concrete bridge deck by means of stress wave techniques, *J. Bridge Eng.* 17 (6) (2012) 847–856.
- [19] A. Zerwer, M.A. Polak, J.C. Santamarina, Detection of surface breaking cracks in concrete members using Rayleigh waves, *J. Environ. Eng. Geophys.* 10 (3) (2005) 295–306.